

Structure of a mitochondrial cytochrome *c* conformer competent for peroxidase activity

Levi J. McClelland^{a,b}, Tung-Chung Mou^{b,c}, Margaret E. Jeakins-Cooley^{a,b}, Stephen R. Sprang^{b,c}, and Bruce E. Bowler^{a,b,1}

^aDepartment of Chemistry and Biochemistry, ^bCenter for Biomolecular Structure and Dynamics, and ^cDivision of Biological Sciences, University of Montana, Missoula, MT 59812

Edited by Harry B. Gray, California Institute of Technology, Pasadena, CA, and approved March 27, 2014 (received for review December 20, 2013)

At the onset of apoptosis, the peroxidation of cardiolipin at the inner mitochondrial membrane by cytochrome *c* requires an open coordination site on the heme. We report a 1.45-Å resolution structure of yeast iso-1-cytochrome *c* with the Met80 heme ligand swung out of the heme crevice and replaced by a water molecule. This conformational change requires modest adjustments to the main chain of the heme crevice loop and is facilitated by a trimethyllysine 72-to-alanine mutation. This mutation also enhances the peroxidase activity of iso-1-cytochrome *c*. The structure shows a buried water channel capable of facilitating peroxide access to the active site and of moving protons produced during peroxidase activity to the protein surface. Alternate positions of the side chain of Arg38 appear to mediate opening and closing of the buried water channel. In addition, two buried water molecules can adopt alternate positions that change the network of hydrogen bonds in the buried water channel. Taken together, these observations suggest that low and high proton conductivity states may mediate peroxidase function. Comparison of yeast and mammalian cytochrome *c* sequences, in the context of the steric factors that permit opening of the heme crevice, suggests that higher organisms have evolved to inhibit peroxidase activity, providing a more stringent barrier to the onset of apoptosis.

Mitochondrial cytochrome *c* (Cyt_c) plays a pivotal role in energy storage in living organisms, providing a critical link between complex III and complex IV of the electron transport chain (1). More recently, the role of Cyt_c as an initiator of the intrinsic pathway of apoptosis has been elucidated (2). Release of Cyt_c from mitochondria into the cytoplasm is a conserved step in apoptosis from yeast up through mammals (3). However, subsequent assembly with Apaf-1 to form the apoptosome is unique to metazoan animals (4, 5). Mitochondrial cytochromes *c* contain a *c*-type heme with axial His18 and Met80 ligands (6). However, when Cyt_c binds to the inner mitochondrial membrane lipid cardiolipin (CL), Met80 ligation is lost (7, 8). In this state, Cyt_c catalyzes CL peroxidation, which provides an early signal for initiation of apoptosis (7).

Despite advances in our understanding of the role of Cyt_c in apoptosis, our knowledge of the structural factors that facilitate the peroxidase activity of Cyt_c remains rudimentary. In the structure of a domain-swapped dimer of horse Cyt_c, Met80 is replaced by water as a heme ligand (9), causing a fourfold increase in peroxidase activity relative to monomeric Cyt_c (10). However, evidence for dimerization of Cyt_c on CL vesicles is lacking. Fluorescence methods provide evidence for an equilibrium between compact and extended conformers on the surface of CL vesicles (11–13), with the extended conformer linked to higher peroxidase activity (13). However, other studies suggest that compact conformers of Cyt_c are also competent for peroxidase activity (14).

The heme crevice loop of Cyt_c (residues 70–85) is the most highly conserved segment of the primary structure of Cyt_c (15, 16). This surface loop contains the Met80 heme ligand and is likely important for both electron transfer function in electron transport and peroxidase activity in apoptosis. Our knowledge of the sequence constraints operating in the heme crevice loop that

modulate the dynamics necessary for peroxidase activity remains sparse. We have shown recently that the dynamics of the heme crevice loop are enhanced when lysine 72 of yeast iso-1-cytochrome *c* (iso-1-Cyt_c) is mutated to alanine (17, 18). When synthesized in its native host (*Saccharomyces cerevisiae*), but not in a heterologous *Escherichia coli* expression system, lysine 72 of iso-1-Cyt_c is trimethylated (tmK72) (19). Structural studies on yeast-expressed iso-1-Cyt_c (hereafter tmK72Cyt_c[Sc]) show that tmK72 lies across the surface of the heme crevice loop (20). Here we show by high-resolution X-ray crystallography that mutation of lysine 72 to alanine produces a variant of iso-1-Cyt_c (hereafter K72ACyt_c[Sc]) that permits ejection of Met80 from the heme-binding pocket and its replacement by water. An extensive buried water channel results, a feature required for substrate access to the heme active site (14, 21) and for proton transport away from the active site during catalysis. As anticipated from the crystal structure, we show that mutation of residue 72 to alanine (K72ACyt_c[Sc] variant) enhances peroxidase activity of iso-1-Cyt_c near physiological pH.

Results and Discussion

Crystallization of K72ACyt_c[Sc]. The K72A variant of yeast iso-1-Cyt_c, K72ACyt_c[Sc], was expressed from *E. coli* (19, 22). This variant carries an additional C102S mutation to eliminate disulfide dimerization (23). Crystals of oxidized (Fe³⁺-heme) K72ACyt_c[Sc] grown from 90% saturated ammonium sulfate at pH 8.8 diffracted to 1.45 Å. Refinement yielded a structural model with $R_{\text{work}}/R_{\text{free}} = 0.145/0.156$ (Table S1). Two molecules of K72ACyt_c[Sc] (chains A and B) are contained in the asymmetric unit of the crystal lattice. The rmsd between chains

Significance

Cytochrome *c* is essential to two important biochemical pathways, the electron transport chain and the intrinsic pathway of apoptosis. The heme crevice loop, which provides the Met80 ligand to the heme cofactor, is the most highly conserved segment of the cytochrome *c* sequence. The dynamics of this loop are likely important for both functions. Cytochrome *c*-mediated peroxidation of cardiolipin in the inner mitochondrial membrane is an early signal in apoptosis. We show that mutation of trimethyllysine 72 to alanine in yeast iso-1-cytochrome *c* allows formation of a conformer of the protein with Met80 displaced from the heme and enhances peroxidase activity. Thus, this residue is likely an important modulator of the peroxidase function of cytochrome *c*.

Author contributions: L.J.M., T.-C.M., S.R.S., and B.E.B. designed research; L.J.M., T.-C.M., and M.E.J.-C. performed research; L.J.M., T.-C.M., and M.E.J.-C. analyzed data; and L.J.M., T.-C.M., S.R.S., and B.E.B. wrote the paper.

The authors declare no conflict of interest.

This article is a PNAS Direct Submission.

Data deposition: The crystallography, atomic coordinates, and structure factors reported in this paper have been deposited in the Protein Data Bank, www.pdb.org (PDB ID code 4MU8).

¹To whom correspondence should be addressed. E-mail: bruce.bowler@umontana.edu.

This article contains supporting information online at www.pnas.org/lookup/suppl/doi:10.1073/pnas.1323828111/-DCSupplemental.

A and B is 0.25 Å. Heme proteins are susceptible to reduction to the Fe(II) state by synchrotron radiation (24). Therefore, we cannot eliminate the possibility that some reduction of the K72ACytc[Sc] heme occurs during data collection. However, treatment of crystals with sodium dithionite leads to crystal cracking, which is not observed following data collection. Also, because the data were collected at 100 K, large structural rearrangements due to heme reduction should be minimal.

Structural Consequences of the Trimethyllysine 72-to-Alanine Substitution. The structure of K72ACytc[Sc] superimposed on that of oxidized tmK72Cytc[Sc] crystallized near pH 6.5 (20) shows that the two proteins are quite similar (rmsd at C_{α} positions: 0.64 Å) (Fig. 1). The key difference is that Met80 has swung out of the heme crevice in K72ACytc[Sc] (Fig. 1A). Most previous structures of monomeric mitochondrial cytochromes *c* have Met80 bound to the heme iron (6). Exceptions include NMR structures of an alkaline conformer of K79ACytc[Sc] obtained at pH 10 where Met80 is displaced by Lys73 (25) and of horse Cytc and an M80A variant of iso-1-Cytc with exogenous ligands bound in place of Met80 (26–28). In K72ACytc[Sc], water (W)113 (probably hydroxide at pH 8.8) is bound to the heme iron in place of Met80. The Fe–O distance of 2.00 Å is similar to that observed in the oxidized (Fe³⁺–heme) horse Cytc domain-swapped dimer and trimer structures (~2.10 Å) (9) and the 2.01-Å Fe–O distance observed for two *Geobacter sulfurreducens* chemotaxis protein sensor domains (29). The presence of H₂O/OH[−] as the axial ligand in place of Met80 does not affect the Fe–N bond distance (2.04 Å) of the transaxial His18 ligand, and is similar to that of tmK72Cytc[Sc] (Fig. S14) and to the Fe–N bond distance of 2.0–2.1 Å observed for *c*-type cytochromes with a water bound *trans*

to the histidine of an Fe³⁺–heme (9, 29). The orientation of the plane of the imidazole ring of His18 remains typical of *c*-type cytochromes (30) and is indistinguishable from that in tmK72Cytc[Sc] (Fig. S14). Three more buried water molecules are located on the Met80-proximal side of the heme. Two of these waters sit near positions occupied by the C_{β} and C_{γ} atoms of Met80 in the tmK72Cytc[Sc] structure (Fig. 1B and Movie S1) and have well-defined electron density (Fig. 1C).

Alternate Side-Chain Conformers and Buried Water Channels in K72ACytc[Sc]. In oxidized tmK72Cytc[Sc], all residues are modeled as single conformers (20). However, in K72ACytc[Sc], several residues occupy two conformations (Table S2). Three of these residues, Asn52, Met64, and Leu85, are fully buried and pack against the heme (Fig. S2). Thus, invasion of water into the heme crevice when Met80 ligation is lost creates disorder around the heme. Both conformations of Asn52 can hydrogen-bond to W119, which is also hydrogen-bonded to Tyr67 (Fig. S14). Two waters, W111 and W116, near the heme also adopt alternate high (~80%) and low (~20%) occupancy positions displaced from each other by 0.67 Å and 1.45 Å, respectively (Fig. 1B and Table S2). In their high occupancy positions, these two waters form a hydrogen-bonded chain emanating from the axial H₂O/OH[−] heme ligand (Fig. 2A). In the low occupancy state, W116 breaks this chain and forms alternative hydrogen bonds (Fig. 2B and Movie S2). Thus, W111 and W116 could act as a transient proton shuttle in general acid/base catalysis during peroxidative turnover catalyzed by the heme of the K72ACytc[Sc] conformation reported here.

The position of water molecules on the Met80-proximal side of the heme of tmK72Cytc[Sc] is sensitive to the redox state of

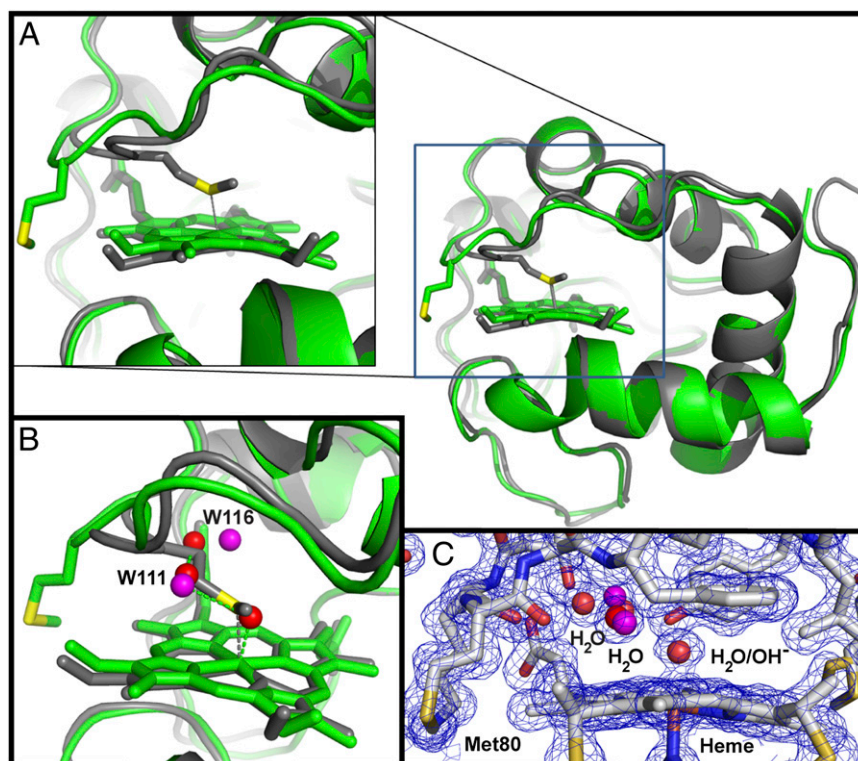


Fig. 1. Comparison of the overall structures of K72ACytc[Sc] and tmK72Cytc[Sc]. (A) Alignment of K72ACytc[Sc] (green; chain A of PDB ID code 4MU8) with tmK72Cytc[Sc] (gray; PDB ID code 2YCC; carries a C102T mutation). The heme and Met80 are shown as stick models. A close-up view of the heme and Met80 is shown (Left). (B) Close-up view of the heme crevice showing waters (red spheres) in K72ACytc[Sc] in the space occupied by Met80 in tmK72Cytc[Sc]. Low occupancy positions observed for two of the waters are shown in purple. (C) Heme crevice close-up view showing the $2|F_o| - |F_c|$ electron density map contoured at 1.2σ (blue wire) with the model used to fit the data.

A versus chain B (Fig. S4), and the pattern of variation of thermal factors near Arg38 is similar to oxidized tmK72Cytc[Sc] for chain A and similar to reduced tmK72Cytc[Sc] for chain B (20). This difference is likely attributable to the presence of sulfate ion interactions with Arg38 in chain A, which are absent in chain B.

Structural Constraints Mediating Ejection of Met80 from the Heme Crevice of Iso-1-Cytc. Relatively small backbone adjustments are sufficient to permit Met80 to swing out of the heme crevice of Cytc (Figs. 1 and 3 and Movie S4). Large displacements occur between the K72ACytc[Sc] and tmK72Cytc[Sc] structures at Met80 (C_{α} rmsd 3.59 Å) and Ala81 (C_{α} rmsd 2.18 Å), and to a lesser extent at Gly83 (C_{α} rmsd 1.26 Å) in the heme crevice loop (Fig. 3A and B). Otherwise, C_{α} rmsd values for alignment of the two structures are mostly <1 Å (Fig. S5). The deviation of the main chain observed here for the heme crevice loop is considerably smaller than when Met80 is expelled from the heme crevice by exogenous ligands such as cyanide (28) and imidazole (27).

Mutation of tmK72→Ala facilitates expulsion of Met80. In tmK72Cytc[Sc], tmK72 sterically blocks movement of Ala81, inhibiting release of Met80 from the heme (Fig. 3A and Movie S3). In horse Cytc, where Lys72 is not trimethylated, a similar situation exists. Lys72 lies across the heme crevice loop, forming hydrogen bonds to the carbonyls of Met80 and Phe82 (34). In K72ACytc[Sc], Ala81 is free to move toward Ala72 as Met80 swings out of the heme crevice (Fig. 3B and Movie S3). Our structural data demonstrate that the more than twofold increase we observe in the dynamics of the His79-mediated alkaline conformational transition of iso-1-Cytc in the presence of the tmK72→Ala mutation (18) results from relaxation of steric constraints in the heme crevice loop.

The most highly conserved portion of the Cytc sequence is the heme crevice loop. It encompasses both tmK72 and the mobile heme ligand, Met80 (15). Within this loop, yeast and mammals differ at positions 81 and 83 (Fig. 3C), two residues that move significantly when Met80 is displaced from the heme crevice. At both positions, more sterically demanding side chains are present in mammalian Cytc than in its yeast counterpart. Phylogenetic analysis shows that ancestral mitochondrial Cytc has alanine at

position 81, as in yeast (35). Moving up the phylogenetic tree from yeast to mammals, position 81 first mutates to Val and then Ile (15, 16). These observations suggest that the heme crevice loop in mammals has evolved to more stringently minimize access to Cytc conformers capable of peroxidase activity than in yeast.

Peroxidase Activity of tmK72Cytc[Sc] Versus K72ACytc[Sc]. To test the effect of the tmK72→Ala mutation on the peroxidase activity of iso-1-Cytc, we compared the rate of oxidation of guaiacol to tetraguaiacol (10, 36, 37) for tmK72Cytc[Sc] versus K72ACytc[Sc] (Fig. S6). At pH 7.5 (Fig. 4A), k_{cat} for peroxidase activity is 35% greater for K72ACytc[Sc] than for tmK72Cytc[Sc]. The pH dependence of k_{cat} shows that peroxidase activity is similar at pH 6 and 6.5 for both proteins (Fig. 4B and Table S3). At these lower pH values, peroxidase activity is expected to be suppressed by the need to deprotonate H_2O_2 (36, 38, 39). However, from pH 7 to 8, k_{cat} for K72ACytc[Sc] increases and remains high, whereas it declines for tmK72Cytc[Sc]. The pH dependence of the peroxidase activity of the yeast-expressed iso-1-Cytc, tmK72Cytc[Sc], mirrors that of horse Cytc (36), relatively constant below about pH 7 and then decreasing at higher pH. The similarity in the pH dependence of yeast and horse cytochromes *c* likely reflects the similar ordering of substructure stabilities for the two proteins (22, 40, 41).

At pH 8, the tmK72→Ala mutation leads to an enhancement of k_{cat} by twofold (Fig. 4B). Furthermore, we observe that crystals of K72ACytc[Sc] crack and dissolve below pH 7, also suggesting that the Cytc conformer observed in the K72ACytc[Sc] structure is less stable at lower pH. Accordingly, the tmK72→Ala mutation favors a Cytc conformer with higher peroxidase activity above pH 6.5.

In mitochondria, the fatty acid chains of CL, which are subject to peroxidation, are believed to bind near Asn52 (site C) and lysines 72, 73, and 86 (site A) (42, 43). The channel of waters that fill the void left when Met80 is expelled could readily be displaced by a fatty acid chain entering from either site A or site C. The side chains of Asn52, Met64, and Leu85 also occupy two rotamers, indicating conformational plasticity on the Met80-proximal side of the heme that could facilitate binding of CL near the heme iron.

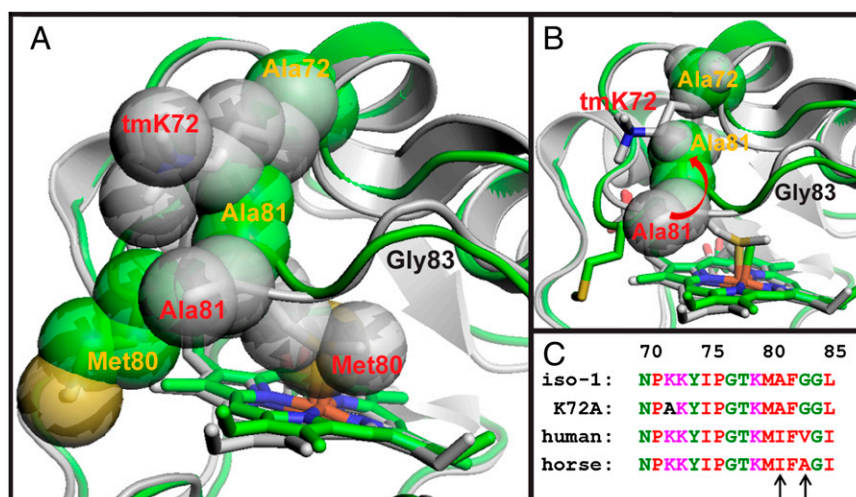


Fig. 3. Steric stabilization of the native conformer of Cytc by the residue at position 72. (A) Overlay of the structures of K72ACytc[Sc] (green, yellow labels) and tmK72Cytc[Sc] (gray, red labels) with residues 72, 80, and 81 shown as space-filling models. The portion of the backbone corresponding to Gly83 is indicated with a black label. (B) Overlay of K72ACytc[Sc] and tmK72Cytc[Sc] showing the movement of Ala81 toward Ala72 when Met80 swings out of the heme crevice. (C) Alignment of yeast and mammalian Cytc sequences for the highly conserved heme crevice loop (residues 70–85). Residues 81 and 83 are marked with black arrows.

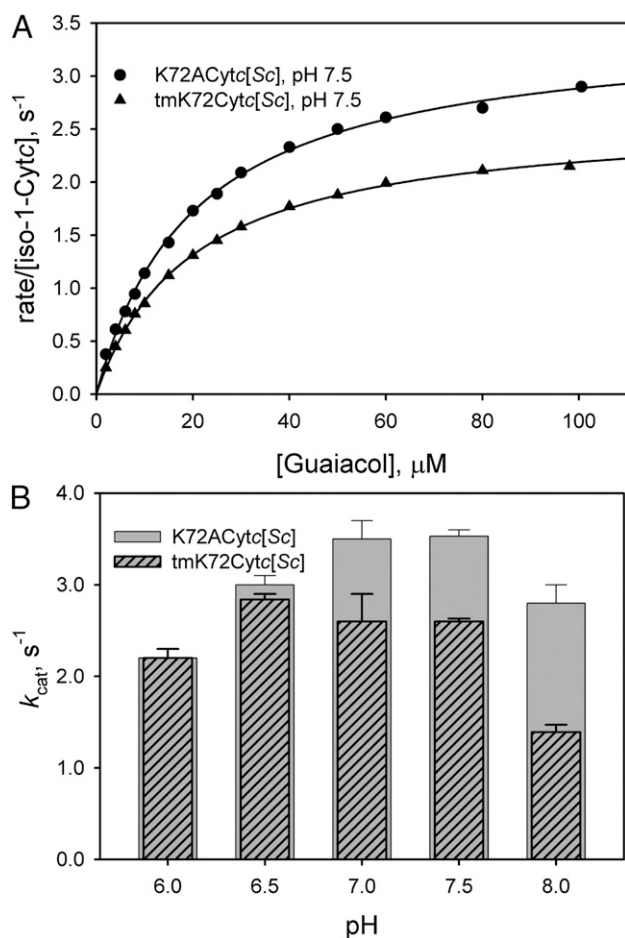


Fig. 4. Effect of the tmK72→Ala mutation on the peroxidase activity of iso-1-Cytc. (A) Michaelis–Menten plots of rate of consumption of guaiacol as a function of guaiacol concentration at 25 °C and pH 7.5 in 50 mM potassium phosphate buffer. Cytc concentration was 1 μM , and H_2O_2 concentration was 50 mM. (B) Plot of k_{cat} (average of three independent experiments with SD) versus pH for K72ACytc[Sc] and tmK72Cytc[Sc].

The peroxidase activity enhancement we observe compares well in magnitude to the increase in the dynamics of the His79-mediated alkaline conformational transition resulting from the tmK72→Ala mutation (18). Thus, residue 72 in the heme crevice

loop significantly impacts the heme crevice dynamics necessary for peroxidase activity. Notably, k_{cat} for the peroxidase activity of horse Cytc at pH 7 (10) determined under identical conditions is 20-fold and 27-fold less than for tmK72Cytc[Sc] and K72ACytc[Sc], respectively (Table S3). The additional steric congestion at positions 81 and 83 (Fig. 3C), in addition to the hydrogen-bond contacts that Lys72 makes with the Met80 and Phe82 carbonyls in mammalian Cytc (34), appears to diminish the heme crevice dynamics needed for peroxidase activity for mammalian versus yeast Cytc. We suggest that Cytc in higher organisms has evolved to limit peroxidase activity, leading to stress-induced release of Cytc from mitochondria, thereby imposing a more stringent barrier to the onset of apoptosis.

Methods

Protein Expression and Purification. Expression of tmKCytc[Sc] was from *S. cerevisiae* GM-3C-2 cells (44) carrying the pRS425/CYC1 shuttle vector (45). K72ACytc[Sc] was expressed from *E. coli* BL21(DE3) cells carrying the pRbs_BTR1 vector (22), as described previously (18). Both proteins carry a C102S mutation to prevent disulfide dimerization during physical studies (23). K72ACytc[Sc] and tmKCytc[Sc] were purified as previously described (18, 46, 47). The procedures are outlined in brief in *SI Methods*.

Crystallization, Structure Determination, and Refinement. A 1:1 mixture of oxidized K72ACytc[Sc] iso-1-Cytc at ~6 mg/mL in 75% aqueous ammonium sulfate and a reservoir solution of 90% ammonium sulfate, 0.1 M Tris-HCl (pH 8.8), and 4% *tert*-butanol was crystallized at 20 °C by vapor diffusion from sitting drops. Diffraction data were collected at the Stanford Synchrotron Radiation Lightsources. The structure was solved by molecular replacement and refined to 1.45-Å resolution. The coordinates and structure factors for K72ACytc[Sc] iso-1-Cytc at pH 8.8 have been deposited in the Protein Data Bank (PDB) (www.pdb.org) under ID code 4MU8. A more complete description of procedures may be found in *SI Methods*.

Guaiacol Assay of Peroxidase Activity. Guaiacol assays were performed at 25 °C with an Applied Photophysics SX20 stopped-flow spectrophotometer. Peroxidase activity was monitored as the formation of tetraguaiacol at 470 nm. The rate of change of absorbance at 470 nm was converted to micromoles guaiacol consumed per second using an absorption coefficient of 26.6 $\text{mM}^{-1}\text{cm}^{-1}$ for tetraguaiacol (36, 37). Michaelis–Menten plots were then used to extract k_{cat} and K_m for guaiacol from the data. Additional details on experimental procedures are provided in *SI Methods*.

ACKNOWLEDGMENTS. This work was supported by grants from the National Science Foundation (CHE-0910616 and CHE-1306903). The Macromolecular X-ray Diffraction Core Facility at the University of Montana was supported by a Centers of Biomedical Research Excellence grant from the National Institute of General Medical Sciences (P20GM10356). The Bruker microflex MALDI-TOF mass spectrometer was purchased with a grant from the National Science Foundation (CHE-1039814).

- Winge DR (2012) Sealing the mitochondrial respirasome. *Mol Cell Biol* 32(14):2647–2652.
- Ow YP, Green DR, Hao Z, Mak TW (2008) Cytochrome c: Functions beyond respiration. *Nat Rev Mol Cell Biol* 9(7):532–542.
- Laun P, Buettner S, Rinnerthaler M, Burhans WC, Breitenbach M (2012) Yeast aging and apoptosis. *Aging Research in Yeast, Subcellular Biochemistry*, eds Breitenbach M, Jazwinski SM, Laun P (Springer, Dordrecht, The Netherlands), Vol 57, pp 207–232.
- Yu T, Wang X, Purring-Koch C, Wei Y, McLendon GL (2001) A mutational epitope for cytochrome c binding to the apoptosis protease activation factor-1. *J Biol Chem* 276(16):13034–13038.
- Olteanu A, et al. (2003) Stability and apoptotic activity of recombinant human cytochrome c. *Biochem Biophys Res Commun* 312(3):733–740.
- Brayer GD, Murphy MEP (1996) Structural studies of eukaryotic cytochromes c. *Cytochrome c: A Multidisciplinary Approach*, eds Scott RA, Mauk AG (University Science Books, Sausalito, CA), pp 103–166.
- Kagan VE, et al. (2005) Cytochrome c acts as a cardiolipin oxygenase required for release of proapoptotic factors. *Nat Chem Biol* 1(4):223–232.
- Kapetanaki SM, et al. (2009) Interaction of carbon monoxide with the apoptosis-inducing cytochrome c-cardiolipin complex. *Biochemistry* 48(7):1613–1619.
- Hirota S, et al. (2010) Cytochrome c polymerization by successive domain swapping at the C-terminal helix. *Proc Natl Acad Sci USA* 107(29):12854–12859.
- Wang Z, Matsuo T, Nagao S, Hirota S (2011) Peroxidase activity enhancement of horse cytochrome c by dimerization. *Org Biomol Chem* 9(13):4766–4769.
- Muenzner J, Toffey JR, Hong Y, Pletneva EV (2013) Becoming a peroxidase: Cardiolipin-induced unfolding of cytochrome c. *J Phys Chem B* 117(42):12878–12886.
- Hong Y, Muenzner J, Grimm SK, Pletneva EV (2012) Origin of the conformational heterogeneity of cardiolipin-bound cytochrome c. *J Am Chem Soc* 134(45):18713–18723.
- Hanske J, et al. (2012) Conformational properties of cardiolipin-bound cytochrome c. *Proc Natl Acad Sci USA* 109(1):125–130.
- Belikova NA, et al. (2006) Peroxidase activity and structural transitions of cytochrome c bound to cardiolipin-containing membranes. *Biochemistry* 45(15):4998–5009.
- Banci L, Bertini I, Rosato A, Varani G (1999) Mitochondrial cytochromes c: A comparative analysis. *J Biol Inorg Chem* 4(6):824–837.
- Moore GR, Pettigrew GW (1990) *Cytochromes c: Evolutionary, Structural and Physicochemical Aspects* (Springer, New York).
- Cherney MM, Junior CC, Bergquist BB, Bowler BE (2013) Dynamics of the His79-heme alkaline transition of yeast iso-1-cytochrome c probed by conformationally gated electron transfer with Co(II)bis(terpyridine). *J Am Chem Soc* 135(34):12772–12782.
- Cherney MM, Junior CC, Bowler BE (2013) Mutation of trimethyllysine 72 to alanine enhances His79-heme-mediated dynamics of iso-1-cytochrome c. *Biochemistry* 52(5):837–846.
- Pollock WB, Rosell FI, Twitchett MB, Dumont ME, Mauk AG (1998) Bacterial expression of a mitochondrial cytochrome c. Trimethylation of Lys72 in yeast iso-1-cytochrome c and the alkaline conformational transition. *Biochemistry* 37(17):6124–6131.
- Berghuis AM, Brayer GD (1992) Oxidation state-dependent conformational changes in cytochrome c. *J Mol Biol* 223(4):959–976.

21. Bortolotti CA, et al. (2012) The reversible opening of water channels in cytochrome *c* modulates the heme iron reduction potential. *J Am Chem Soc* 134(33):13670–13678.
22. Duncan MG, Williams MD, Bowler BE (2009) Compressing the free energy range of substructure stabilities in iso-1-cytochrome *c*. *Protein Sci* 18(6):1155–1164.
23. Cutler RL, Pielak GJ, Mauk AG, Smith M (1987) Replacement of cysteine-107 of *Saccharomyces cerevisiae* iso-1-cytochrome *c* with threonine: Improved stability of the mutant protein. *Protein Eng* 1(2):95–99.
24. Can M, et al. (2013) Structural characterization of *Nitrosomonas europaea* cytochrome *c*-552 variants with marked differences in electronic structure. *ChemBioChem* 14(14):1828–1838.
25. Assfalg M, et al. (2003) Structural model for an alkaline form of ferricytochrome *c*. *J Am Chem Soc* 125(10):2913–2922.
26. Banci L, et al. (1995) Three-dimensional solution structure of the cyanide adduct of a Met80Ala variant of *Saccharomyces cerevisiae* iso-1-cytochrome *c*. Identification of ligand-residue interactions in the distal heme cavity. *Biochemistry* 34(36):11385–11398.
27. Banci L, et al. (2001) Effects of extrinsic imidazole ligation on the molecular and electronic structure of cytochrome *c*. *J Biol Inorg Chem* 6(5-6):628–637.
28. Yao Y, et al. (2002) Solution structure of cyanoferricytochrome *c*: Ligand-controlled conformational flexibility and electronic structure of the heme moiety. *J Biol Inorg Chem* 7(4-5):539–547.
29. Pokkuluri PR, et al. (2008) Structures and solution properties of two novel periplasmic sensor domains with *c*-type heme from chemotaxis proteins of *Geobacter sulfurreducens*: Implications for signal transduction. *J Mol Biol* 377(5):1498–1517.
30. Bren KL, Kellogg JA, Kaur R, Wen X (2004) Folding, conformational changes, and dynamics of cytochromes *c* probed by NMR spectroscopy. *Inorg Chem* 43(25):7934–7944.
31. Louie GV, Brayer GD (1990) High-resolution refinement of yeast iso-1-cytochrome *c* and comparisons with other eukaryotic cytochromes *c*. *J Mol Biol* 214(2):527–555.
32. Lo TP, Komar-Panicucci S, Sherman F, McLendon G, Brayer GD (1995) Structural and functional effects of multiple mutations at distal sites in cytochrome *c*. *Biochemistry* 34(15):5259–5268.
33. Cutler RL, et al. (1989) Role of arginine-38 in regulation of the cytochrome *c* oxidation-reduction equilibrium. *Biochemistry* 28(8):3188–3197.
34. Bushnell GW, Louie GV, Brayer GD (1990) High-resolution three-dimensional structure of horse heart cytochrome *c*. *J Mol Biol* 214(2):585–595.
35. Fitch WM (1976) The molecular evolution of cytochrome *c* in eukaryotes. *J Mol Evol* 8(1):13–40.
36. Diederix REM, Ubbink M, Canters GW (2001) The peroxidase activity of cytochrome *c*-550 from *Paracoccus versutus*. *Eur J Biochem* 268(15):4207–4216.
37. DePillis GD, Sishita BP, Mauk AG, Ortiz de Montellano PR (1991) Small substrates and cytochrome *c* are oxidized at different sites of cytochrome *c* peroxidase. *J Biol Chem* 266(29):19334–19341.
38. Diederix REM, Ubbink M, Canters GW (2002) Peroxidase activity as a tool for studying the folding of *c*-type cytochromes. *Biochemistry* 41(43):13067–13077.
39. Diederix REM, Ubbink M, Canters GW (2002) Effect of the protein matrix of cytochrome *c* in suppressing the inherent peroxidase activity of its heme prosthetic group. *ChemBioChem* 3(1):110–112.
40. Krishna MM, Lin Y, Rumbley JN, Englander SW (2003) Cooperative omega loops in cytochrome *c*: Role in folding and function. *J Mol Biol* 331(1):29–36.
41. Bai Y, Sosnick TR, Mayne L, Englander SW (1995) Protein folding intermediates: Native-state hydrogen exchange. *Science* 269(5221):192–197.
42. Kalanxhi E, Wallace CJA (2007) Cytochrome *c* impaled: Investigation of the extended lipid anchorage of a soluble protein to mitochondrial membrane models. *Biochem J* 407(2):179–187.
43. Sinibaldi F, et al. (2010) Extended cardiolipin anchorage to cytochrome *c*: A model for protein-mitochondrial membrane binding. *J Biol Inorg Chem* 15(5):689–700.
44. Faye G, Leung DW, Tatchell K, Hall BD, Smith M (1981) Deletion mapping of sequences essential for in vivo transcription of the iso-1-cytochrome *c* gene. *Proc Natl Acad Sci USA* 78(4):2258–2262.
45. Herrmann LM, Flatt P, Bowler BE (1996) Site-directed replacement of the invariant lysine 73 of *Saccharomyces cerevisiae* iso-1-cytochrome *c* with all ribosomally encoded amino acids. *Inorg Chim Acta* 242(1-2):97–103.
46. Redzic JS, Bowler BE (2005) Role of hydrogen bond networks and dynamics in positive and negative cooperative stabilization of a protein. *Biochemistry* 44(8):2900–2908.
47. Wandschneider E, Hammack BN, Bowler BE (2003) Evaluation of cooperative interactions between substructures of iso-1-cytochrome *c* using double mutant cycles. *Biochemistry* 42(36):10659–10666.